LASER INDUCED PLASMA ABLATION

OF BIOLOGICAL TISSUE

by

JILL M. TOBIN

SUBMITTED TO THE DEPARTMENT OF
PHYSICS IN PARTIAL FULFILLMENT OF THE
REQUIREMENTS FOR THE
DEGREE OF

BACHELOR OF SCIENCE

at the

MASSSACHUSETTS INSTITUTE OF TECHNOLOGY

June 1985

Massachusetts Institute of Technology 1985

Signature of
Author_____
Department of Physics
May 17, 1985

Certified by_____
Dr. Michael S. Feld
Thesis Supervisor

Certified by_____
Carter Kittrell
Thesis Supervisor

Accepted by_____
Dr. Malcolm Strandberg
Chairman, Department Committee

ABSTRACT

A Q-switched Nd:YAG laser radiation was brought to a tight focus to induce optical breakdown of biological materials including calcified plaque and bone. There appeared to be no peripheral thermal damage around the target site. The process was capable of ablating precise amounts of tissue. A quantitative analysis of the amount of tissue removed for varied user-controllable parameters such as incident power and focal region diameter, number of pulses delivered and wavelength was made. The YAG fundamental (1064nm), as well as second and fourth harmonic radiation (532nm and 266nm), were used in this study. The physical processes responsible for the initiation, growth and control of the induced plasma and subsequent material damage are discussed.

TABLE OF CONTENTS

ACKNOWLEDGEMENTS

I. INTRODUCTION

There is a growing interest in medical applications of lasers, particlularly in the field of cardiology. Lasers may be employed as a technique for removing atherosclerotic plaque from plaqued arteries. Such a treatment would be an alternative to coronary bypass surgery and balloon angioplasty. Approximately 170,000 coronary bypasses are performed annually.(1.) This operation requires the chest to be opened and a healthy vein from elsewhere in the patient's body to be grafted around the blocked artery so as to provide an alternate route for blood flow. The laser treatment would not require extensive surgery. Instead a catheter containing optical fibers would be introduced into the patient's artery. The catheter would be positioned at the occlusion and a predetermined amount of laser energy would be delivered to the diseased site to vaporize the blockage.

Current research is directed at understanding the tissue removal mechanism, and choosing a laser system matched to the desired clinical effect. The desirable effects include: minimizing unwanted deposition of heat in surrounding tissue, the selective removal of tissue, and maximizing of the efficiency of the process. Essentially, there are three different laser induced mechanisms known to cause tissue

ablation. These are: thermal heating leading to vaporization of the tissue water, and recently UV photochemical dissociation, and plasma ablation. These three mechanisms are associated with three different laser systems. Also, the ablated areas produced are characteristic of the mechanism employed. This thesis presents the plasma ablation mechanism as an effective processes for the removal of both hard and soft tissue.

Most recent work in laser treatment of atherosclerosis has employed the thermal mechanism for tissue removal by utilizing the argon ion laser. This laser is a continuous wave (CW) gas laser that is usually operated in the visible wavelengths 514nm and 488nm, and other weaker lines (blue-green) Commercially available optical fibers can conduct radiation at these wavelengths.

It has been demonstrated that the argon ion laser is successful in vaporizing a variety of tissues including certain atheromas.(2)(3) However, the greatest problem associated with its use is the high incidence of arterial perforation. Also, it appears that argon ion radiation is not effective in removing calcified lesions.(4) Laser induced heating of calcified lesions seem to cause the substance to become vitrified. The thermal mechanism associated with tissue removal by argon radiation may be

ineffective in treating hardened tissues at all. This
mechanism appears to work to a large extent by vaporizing
tissue water, and is not capable of generating the
temperatures required to ablate hardened material. These
problems are the motivation for this thesis which
investigates an alternate mechanism for tissue removal.

Two laser systems are of special interest because they
are capable of removing tissue by a nonthermal process.
These are the Q-switched Nd:YAG and the excimer laser. While
this thesis is concerned principally with the use of Nd:YAG
radiation, a number of researchers are currently
investigating the use of excimer laser radiation for ablating
tissue.(5,6) This laser provides UV radiation at a number of
wavelengths. Studies performed on the cornea and on skin has
shown that it is possible to remove thin layers of tissue.
The damage area appears smooth with minimal peripheral
denaturation of the tissue. It has been speculated that the
mechanism responsible is primarily photodissociation of the
constituents of the tissue by the energenic UV photons.
However, it is still unclear whether other mechanisms are
active.

Our initial studies in both soft and hard tissue samples
demonstrated that focused Q-switched Nd:YAG radiation
(1064nm) and its harmonics (532nm, 266nm) produce a plasma at

the target site. The resulting damage appears "clean", with minimal thermal denaturation of surrounding tissue similar to what has been observed with UV excimer radation. These observations indicate that mechanisms (which may include photodissociation) other than simple thermal heating of the water contained in the tissue are active in the ablation process. These mechanisms are capable of removing hard materials (ie. calcified plaque). It was also shown that plasma formation leading to tissue damage can be acheved using visible or infrared radiation. This raises questions about the claimed importance of UV photons (inducing photochemical effects) in ablating tissue without accompanying thermal effects.(6,7) Use of YAG laser radiation rather than excimer light would mitigate the question of mutagenicity of the laser radiation, which surrounds work done in the UV. The YAG laser would also provide wavelengths at which practical optical fibers are readily available.

This thesis presents quantitative data establishing minimum fluence theresholds and hole size, plus qualitative observations concerning peripheral damage at various wavelengths, energy densities, and incident spot sizes. Experiments were carried out using cadaver plaque samples as well as various other materials. Organic and inorganic target materials were used to further an understanding of the

mechanisms involved and allowed for repetitive studies to be performed, as the supply of cadaver samples was limited.

There are two characteristics of plasma ablation that make it obviously different from other mechanisms. First, the plasma acts as an intermediary in the coupling of the laser light to the tissue sample. Secondly, the temperatures achieved in the focal region are capable of vaporizing materials that can not be vaporized by usual thermal heating. From previous studies of laser induced plasma formation in inorganic solids, several different mechanisms for plasma initiation and growth have been identified. It is not yet known which of these (if any) are dominant in plasma removal of tissue. I can only suggest which may be active and their relative importance at this time. A complete understanding of the physical processes involved will require further experimentation. I have suggested a few areas for future investigation in my closing statements. I hope that the data presented here will stimulate interest and lead to further progress.

II. Theory of Optical Breakdown and Plasma Formation

It is well known that focused pulsed laser radiation will produce a plasma in a target medium. This process of producing a plasma was first demonstrated in gases and later in metals and glasses.(7,8) Consequently, theories describing laser induced breakdown began with the consideration of gases and have been extended to explain optical breakdown of liquids and solids. Material damage was immediately associated with optical breakdown and plasma formation. This arose from a common observation noted for almost every medium used: a spark was observed whenever damage occured. Therefore, theories concerning this phenomenon center on 1) how the plasma is initiated and formed, 2) what mechanisms associated with the plasma are active in producing damage in the target material. The consideration of these two aspects attempts to explain the threshold behavior for damage and the nature and extent of the damage itself.

The theory describing laser induced plasmas can be considered in two parts 1) the initiation process of producing free electrons, 2) the net transfer of energy to these electrons so as to induce an avalanche effect enabling the plasma to grow. Obviously, the second step can not occur without the first.

The most likely mechanisms proposed as the cause of the existence of these critical starter electrons are multiphoton ionization enhanced by intraband optical absorption (resonance enhanced multiphoton ionization), and thermionic emission enhanced by absorbing imperfections and inclusions present in the sample.

Thermionic emission is ionization caused by intense focal heating of the target. Q-switched lasers deliver pulses of radiation of high peak intensity and short duration. The high intensity enables conduction electrons to gain energy faster than they lose it to the material surface. Temperatures as high as twenty thousand degrees C exist at the focal spot.(9) This results in an emission of electrons and ions. Secondly, the focussing of this radiation creates an energy density that assures that a critical number of emissions occur within the time of one pulse. Since the total energy in a pulse is relatively low, general thermal heating of the material becomes an unimportant process. Small solid impurities in the focal region may absorb enough energy to become extremely hot. Local breakdowns or explosions occur at these points liberating ions and electrons.(10)

In general, surfaces tend to have a lower threshold for damage than bulk material. Some authors attribute this to

chemical contamination of the surface (ie. dust particles, grease spots). It was demonstrated that carefully cleaned surfaces by argon ion beam bombardment and evaporation in vacuum caused the threshold to be raised significantly.(11) Even so, these surfaces still had a lower threshold than the bulk material. Bloembergen asserts that this is due to the presence of physical imperfections at the surface such as grooves, scratches, cracks and pores.(12) He calculates by means of electrostatics the electric field configuration in the neighborhood of these imperfections. Near the edges there is a concentration of the lines of force which will initiate breakdown.

Multiphoton processes are most likely responsible for the initial ionizations especially at short wavelengths.(13) In Fig 1, three multiphoton schemes are illustrated. Figure a) while being unlikely to occur in reality, illustrates the conceptual basis for deriving the probability of multiphoton transitions occurring. In figure b), an ionization occurs due to the simultaneous absorption of n photons. n is the integer greater than $I_o/h\nu$. Where I_o is the ionization potential and $h\nu$ equals the photon energy. The probability of a 10 photon transition occuring (required for ionization by IR radiation) is clearly less likely than a 3 photon (UV) transition.

It is generally agreed upon that the growth of the plasma is due to an electron cascade or avalanche. N. Bloembergen first identified the electron avalanche process as being the principal mechanism after comparing his observations of breakdown in gases using 1.06μm and 0.69μm radiation to that of dc breakdown. He found the two nearly identical.(14) The theory of avalanche breakdown known as inverse bremsstrahlung may be described as follows:

Once free electrons are present in the focal region they may acquire enough energy from the oscillating electric field of the laser radiation to cause ionization through collisions. By a classical treatment of an electron in an oscillating electric field, a laser fluence (J/cm^2) required to increase the number of electrons from a few free electrons to 10^{16} electrons per cm^3, constituting a plasma, can be derived. This type of derivation can give only an order of magnitude estimate because losses have been ignored. A proper treatment should include losses due to diffusion of electrons out of the focal volume, attachement of electrons to form neutral species, and recombination of ions.(15)

Once the plasma is formed it acts to shield the target material from further incoming radiation by absorbing and scattering incoming light. The electrical conductivity of the plasma can be derived. The conductivity is dependent on

the collision frequency. The collision frequency of the plasma may be estimated by first approximating the energy of a free electron in a laser generated plasma (laser intensity $F=10^7 w/cm^2$) as a function of the density of electrons N. Placing this into the formula for the conductivity, one can see that as N increases the conductivity decreases. The typical laser frequency used is about 10^{15}hz. When ω is greater than or approximately equal to ν_c then light is transmitted through the plasma to the tissue, the plasma then passes through a period where the incident light is absorbed. If N were allowed to grow without bound eventually the plasma might become reflecting. The absorption occurs by the inverse bremsstrahlung process described above. The light is scattered by thermally excited acoustic waves. In this process known as Brillouin scattering, the light is also shifted in frequency an amount equal to the frequency of the characteristic phonons of the material. Stimulted Brillouin scattering may also occur where the laser radiation itself acts to create accoustic waves.(16)

There has been considerable investigation of the geometry of plasma growth in gases. It has been noted that once the plasma is formed, it generally spreads from the focal point in an asymmetrical matter. The growth is elongated back towards the laser (17).

The bright spark that is observed is due to excited ion
transitions and energy being released, as photons, as a
result of electrons recombining. UV, visible as well as x-
rays are emitted.(18) It is unclear whether this emission
itself plays a significant role in damaging the material.
Most likely, it is the bombardment of energenic electrons and
ions with the material surface causing further ionizations
and dissociations, the primary means by which tissue is
ablated. It still is unclear whether these collisions result
in dissociations and ionizations, or whether they serve to
further heat the material.

Vaporization and melting of the tissue may occur in the
focal region. The plasma temperatures here have been found
to be as high 15,000°K,(19) However, this temperature is
contained in a highly localized region and the time in which
this temperature is maintained is extremely short. Thus, the
total heat energy deposited in the whole sample is low.
Thus, very little thermal damage appears.

Another process associated with optical breakdown is
the generation of a shock wave. This is most likely due to
the rapid expansion of the plasma (4 km/sec).(20) Also,
stimualted Brillouin scattering, thermal expansion and phase
changes due to thermal heating will generate acoustic waves.
When this wave proagates into the material the tissue

structure is disrupted. This may aid the ablation process, but it may also produce undesireable effects in neighboring tissue structures.

In summary, the level of incident irradiance (W/mm^2), the amount of energy actually deposited in the tissue, the time over which the plasma is sustained, and the physical properties of the tissue determine the size and extent of the damage zone.

III. Experimental Considerations:

Experiments were performed using calcified and fibrous plaque samples taken from sections of human cadaver artery as well as normal human artery (usually the carotid artery), calf aortas, beef bone, and gelatin. While human cadaver samples are the most relevent for this study, it was difficult to obtain consistant samples on a regular basis. Atherosclerotic plaque varies considerably in amount and structure from sample to sample and even within one sample. In order to perform repetitive studies, alternative hard and soft tissue samples were used. Gelatin was used as a model for soft tissue. Since the gelatin mixtures (Knox unflavored gelatin and distilled water) were transparent, non-destructive observations of the damage area, could be made.

Identical experimental procedures were used with all these samples. Figure 2 illustrates the experimental apparatus used with the Nd:YAG laser. A Quanta-Ray (Spectra Physics, Mountainiew CA) Q-switched Nd:YAG laser was used. This laser delivers 10 nsec pulses at 10 Hz. Doubling crystals were used to generate the second (532nm) and fourth (266nm) harmonic radiation. The average power of the laser was monitored using a Scientech (Scientech Inc. Boulder, CO) thermal power meter.

The beam diameter focused and unfocused, was measured by translating a polished sharp silica edged into the beam and monitoring the transmitted power with a photodiode. The beam was brought to a focus using fused silica lenses of 100, 200 and 300 mm focal lengths. This enabled us to produce different incident spot sizes. The pulse shape duration and delivery rate were examined with an FND-100 (EG&G Electro-optics division, Salem, MA) photodiode and a fast oscilloscope.

Samples were mounted on an xyz translator to facilitate positioning the surface of the sample at the focal point. The xy position of the translator across the beam diameter was controlled by an electric motor and belt system. The movement of the translator was synchronized with the pulse delivery rate so that the number of pulses delivered to a particular site could be determined and reproduced in a line. This also enabled us to remove lines and areas of tissue as well as holes.

Sample were exposed to single pulses, series of 3 and 10 pulses and repetitive pulses for 5 and 10 secs at 5 and 10 Hz both in the "hole" configuration (translator stationary) and in the "line" configuration in which the sample is translated across the beam.

The damage area was examined using a dissecting

microsope and a standard microscope. The diameter of the
damged area was measured using a reticle placed in the ocular
of a dissecting microscope. To measure hole depth an Olympus
BH-2 microscope with 100x magnification is focused at both
the top and the bottom of each hole. The fine adjustment
knob been calibrated (200μm/turn) and by reading the
difference in the setting when foccused at the different
planes, depth can be estimated to ±25μm. Photographs were
taken of the samples.

Artery samples were then fixed in formalin solution and
sent to a pathologist (Dr. Burr Ratliff Cleveland Clinic
Foundation) for histologic sectioning. The mounted samples
were analyzed by Dr. Ratliff and returned to MIT. At MIT the
physical dimensions of the damage sites in the histologic
sections were measured and compared to previous optical
measurements. It was found that optical measurement differed
from measurements taken from histology by -6%. This may be
due to shrinkage of the sample during the fixing process.

IV. Observations and Discussion of Results

There are two aspects to the observations made of the
plasma ablation process. The first are qualititative
observations about the nature of the ablation process and of
the target site after it is exposed to the laser radiation.
The second are quantitative measurements of the dimensions of
the ablated site (ie. hole depth and diameter) and how these
relate to the energy supplied and how the energy is supplied
(ie. focused spot, radiation wavelength). Both types of
observations were made in the laboratory and supported by
histology as described in the previous chapter.
Visual observation of the removal process:

With each pulse of the laser a bright spark is seen at
the surface of the sample. The spark is usually yellowish
white, but under careful examination is slightly different
for different samples. Its size is largely determined by
the size of the focal region. The spark is bright enough to
observe in normal room lighting. A snapping sound is
simultaneously heard with each spark produced. Tissue
removal is always accompanied by such a spark.

This process produces circular holes. These circles
are nearly perfect in homogeneous media such as gelatin, and
are slightly irregular in inhomegeneous media. When lines

are prodced the thickness of the groove produced varies by
only 2.5%. The shapes of the holes produced tend to be
pencil-like as illustrated in fig 3. The cross section of a
line is rectangular. (fig 4). The coloring of the inside of
these holes/grooves, and the surrounding area is the same as
the bulk of the sample. Histologic examination reveals that
there is no char or bubble formation around the ablated site.
(fig. 6) These observations were made for both hard and soft
tissue ablation. Certain cadaver plaque samples contained
both fibrous and calcified plaque. It was possible to remove
uniform lines of tissue in such samples. In other words, the
removal process was effective even in highly varied and
complicated plaqued regions.

Quantitative data:

For each sample type, the threshold for optical
breakdown causing tissue ablation was found at each
wavelength (266, 532, 1064nm) for three different incident
spot sizes. The existance of a threshold results from the
nature of non-linear process.(ie. in a certain region a few
percent change in one parameter results in a large gain).
For this reason, there is some ambiguity to the exact value
of the threshold. The following criteria were used in
defining the threshold point. 1) the plasma must be seen and

heard under normal room lighting and noise. 2) The resulting damage depth must be greater than 25μm (capable of being measured optically) 3) The above two criteria be must met in at least 80 out of 100 shots generated for a given set of parameters.

The threshold seems to be dependent on the following parameters: 1) wavelength, 2) incident spot size, 3) type of target material. This threshold is most likely an intensity per unit area. However, since the pulse duration of the Q-switched laser is fixed (20nsec) one can compare energy densities (J/mm^2), which I have chosen to call the "threshold fluence".

When the samples were exposed to fluences above the threshold, the amount of material ablated was the same as that ablated by the threshold fluence. One can visually observe the plasma growing back up the laser beam, absorbing the incident light. Using high laser fluences only makes the process less efficient. Therefore, the effect of varying various parameters on the threshold fluence was investigated.

Figures 7a-c illustrate the threshold fluence dependence on incident laser spot size for given wavelengths and samples. It appears that two regimes exist. In the first regime (smaller incident spot sizes) the threshold fluence decreases with increasing spot size. In the second, the

fluence remains the same with increasing spot size. The

extent of these regimes is determined by the density of "hot

spots" (easily ionized inclusions and impurities, structural

irregularities of the tissue).(21) If the incident area is

small compared to the density of hot spots, the probability

of initiating breakdown is less than that for a spot size

that has the probability of 1 of including a hot spot in its

incident area.(fig. 8) Spot sizes greater than these are

assured an initiation. However, the inclusion of a large

number of hot spots does not lower the threshold

significantly, as a plasma may be initiated from a single

free electron.

In figure 9a, the threshold fluence for a 100μm spot

diameter, is plotted as a function of wavelength. These

fluences were chosen because actual data is available for

this spot size. However, the greatest efficiency may not be

achieved at this spot size. The most efficient fluence

occurs at the smallest incident spot where the curve of

fluence versus spot size (fig 7) has reached its asymptote.

For comparison, the asyptotic fluence was extrapolated from

the experimental data and plotted as a function of

wavelenghth (fig 9b). In general the fluence appears to

decrease with decreasing wavelength.

The conclusion may be drawn that the initiation process

dominates the threshold. First, the threshold observed experimentally is greater than the threshold derived theoretically for ionization which is itself greater than the fluence required for the avalanche process. Secondly, the wavelength dependence found experimentally corresponds to the wavelength functionality of the initiation process, particularly multiphoton ionization, and not to the functional dependence on wavelength of inverse bremsstrahlung, which is inversely proportional to the wavelength squared. Thirdly, the influence of increasing spot size in lowering the threshold, as described above, can serve as evidence for the initiation process as being a dominant mechanism.

The magnitude of the damage area as a function of incident spot size is presented in figures 10a-c. The depth was found to be independent of spot diameter for a given wavelength. The diameter of the ablated area was roughly equal to the incident spot size.

The depth of the ablated area as a function of threshold fluence is graphed in figure 11. Each threshold fluence corresponds to the asymptotic value determined by figures 7a-d for each wavelength. It was found that the depth increases roughly linearly with increasing fluence. Data for beef bone, calf artery and calcified plaque, as well as the

theoretical depth removed per fluence for water vaporization is plotted. The energy density required for the thermal vaporization of one mm^{-3} water is roughly 2.5J.

The fluence required for the removal of one mm   multiplied by the incident area, should equal the volume of tissue removed multiplied by ΔH, the efficiency of ablation. However, this assumes that all of the fluence energy is actually absorbed within the ablated volume. In reality only a fraction enters this region; the rest is lost due to scattering. Therefore, there is also a coefficient α that must also be determined.

$$I A \Delta t_p = \frac{\Delta H}{\alpha} A_a D_a$$

$I \Delta t_p = F$ = laser fluence
  A = incident spot site
$A_a D_a$ = ablated volume

In figure 12, the plasma energy efficiency $\Delta H/\alpha$ is calculated. The efficiency of ablation is greatest for 266nm radiation. At this wavelength the efficiency is even greater that of the thermal vaporization of water (2.5J/mm^3)

Also, the penetration depths in human artery for each wavelength are presented for comparison to the ablated depth resulting from the plasma mechanism. The ablation depths are consistantly less than the penetration depths. It may be concluded that the plasma process always occurs before any thermal mechanism can become active.

Generally, it was found that the fluence thresholds of gelatin did not follow the same trends as the other samples. Also, very large damage areas were produced. Therefore, gelatin can not be regarded as a good model for calcified plaque. However, it did provide the following insights: first, the shape of the ablated hole could be seen in three dimensions. Secondly it was observed that the plasma could be initiated within the sample causing material fragments to be ejected. These fragments may absorb incoming radiation and aid in the shidlding of the material from incoming radiation.

V.   Comparison with Excimer Ablation

This study demonstrates that Q-switched Nd:YAG radiation
causes ablation of biological tissue in a manner that is
markedly different from that induced by continuous wave
lasers, but is not dramatically different from the results of
studies employing excimer radiation. This can seen
immediately by the appearance of the ablated area. The
mechanisms of vaporization and pyrolysis, are associated with
destruction of tissue by continuous wave lasers. The ablated
areas are crater-like holes surrounded by concentric zones of
thermal damage. The excimer 193nm radiation produces smooth
holes without surrounding thermal damage. The most recent
work empolying this laser has recognized that there might be
two mechanisms operative. The first mechanism usually cited
is localized photochemical dissociation of molecular bonds
given sufficient UV photon flux and absorption. The second
mechanism is due to the way in which the radiation is
delivered. The short pulses of the excimer laser may indeed
induce a plasma or fragmentation of the tissue. The
vaporized fragments may remove the energy from the system so
quickly that there is not enought time for significant heat
transfer to the tissue to occur.   Our study employing longer
wavelength radiation in a pulsed mode suggests that it is the

short pulse high intensity delivery of energy that is largely
responsible for producing damage sites in which there is no
thermal injury. Currently, it is not clear whether this is
also the case with excimer ablation of tissue. Spectrocopic
studies must be performed on the emission produced by such UV
radiation. Many researches have noted a threshold phenomenon
for excimer ablation, this threshold should be investigated
further and compared to the thresholds found for Nd:YAG
ablation. Careful attention must be made to the definition
of "threshold" and to the definition of plasma. Although we
do not know to date whether the same or different mechanisms
are active for excimer and YAG ablation, the gross properties
of the damage area can still be compared. The character of
the ablated areas are both free of thermal denaturation.
both mechnisms can remove small, precise amounts of tissue.
However, there may be inherent benefits for using Nd:YAG
radiation. The use of infrared or visible radiation
eliminates the question of the possible mutigenicity of UV
laser light. The Nd:YAG laser has better beam quality
allowing for it to be focused to a smaller spot size. There
are also capital and maintanence cost benefits to the Nd:YAG
system. The most important question yet to be answered is
which system can be used with a fiber optic delivery system.
This question is currently being investigated.

VI. Conclusion

This thesis has presented both qualititative and quantitative data demonstrating that the plasma ablation process is effective in removing both hard and soft tissue. The mechanisms associated with this process have been outlined and some rough estimates of their contribution have been made. Since there are still many unknowns abc·'t this process, a firm conclusion on which process is dominant can not yet be drawn. I have presented three mechanisms: two pertain to the initiation of the plasma, multiphoton ionization and thermionic emission of electrons, and a driving mechanism for the plasma growth, inverse bremsstrahlung. I have suggested that the resulting plasma produces high temperatures in the focal region leading to vaporization of even hard calcified tissue. Damage may also result from electron and ion collisions with the material, the presence of both UV and x ray radiation and shock waves. Clearly, real time diagnostics must be made of the plasma and irradiated area. One may try to detect blackbody radiation resulting from the expected high temperatures. Spectroscopic studies could be performed to look for fluorescence from the intermediate states of the multiphoton process. The plasma density can be probed both in space and time. The results of

such experiments will help to refine our assumptions made in trying to calculate a theoretical threshold, and will lead to a clearer understanding of the process.

In summary, this study demonstrates the precise control over tissue ablation that can be achieved with focused pulsed laser radiation. This precision, combined with the lack of thermal damage to adjacent areas and the ability to remove hardened tissue suggest that such a laser system transmitted through fiber optics could be employed in a variety of medical procedures. Besides the potential vascular use which prompted this study, other applications may include the ablation of bone or cartilage fragments during athroscopy, and the removal of stones and tumors in the biliary or urologic tracts.

FIG 1

MULTIPHOTON PROCESSES

a)

IONIZATION

$|i\rangle$

$h\nu = \hbar\omega$

SIMULTANEOUS
ABSORPTION
OF n PHOTONS

$$P_{if} = (P)^n$$

b)

$|f\rangle$

$|k_2\rangle$

$|k_1\rangle$

$|i\rangle$

$\gamma \rightarrow$

STEP-WISE

$$P_{if} = \gamma$$

c)

$|f\rangle$

$|k\rangle$

$|i\rangle$

γ

(n)

3 photon
resonant
(m)

$$P_{if} \sim (P_1)^m (P_2) \gamma$$

FIG. 2
EXPERIMENTAL SET UP

OSCILLOSCOPE

PHOTO DIODE

XYZ TRANSLATER

MOTOR

BEAM PATH

FOCUSING LENS

THERMAL POWER METER

ATTENUATOR OR BEAM SPLITTER

IRIS

DOUBLING CRYSTALS

Q SWITCHED ND:YAG LASER

FIGURE 4.

SHAPE OF ABLATED HOLE

cross SECTION

TOP VIEW

FIGURE 5

ABLATED LINES OF TISSUE

CROSS SECTION

BOTTOM OF HOLE

TOP VIEW

FIG 6   HISTOLOGY

PLAQUED HUMAN ARTERY
ABLATED BY 1064 nm. RADIATION

PLAQUED HUMAN ARTERY
ABLATED BY 532 nm RADIATION

CALCIFIED PLAQUE

FIG 7A   THRESHOLD FLUENCE
as a function of
INCIDENT SPOT SIZE

FOR 3 WAVELENGTHS

FIG 7

BEEF BONE

FIG 7B   THRESHOLD FLUENCE
as a function of
INCIDENT SPOT SIZE

FOR 3 WAVELENGTHS

FIG 7C

THRESHOLD FLUENCE
as a function of
INCIDENT SPOT SIZE
for 3 wavelengths

CALF ARTERY

THRESHOLD FLUENCE

0.5
0.4 — 1064 nm
0.3
0.2
0.1 — 532 nm
— 266 nm

0   1   2   3   4   5   6 $\pi \times 10^{-2}$
mm

INCIDENT SPOT AREA

FIG 8

THRESHOLD FLUENCE (for a 100 μm spot diameter) as a function of WAVELENGTH for 4 samples

FIG 9   THRESHOLD FLUENCE
(ASYMPTOTIC VALUE)
VS
WAVELENGTH

for 4 samples

FIG 10A
ABLATED DEPTH AND DIAMETER
FOR DIFFERENT
INCIDENT SPOT SIZES

BEEF BONE

$\lambda = 1064\,nm$

INCIDENT SPOT DIAMETER

$\lambda = 532\,nm$

DIAMETER

DEPTH

INCIDENT SPOT DIAMETER
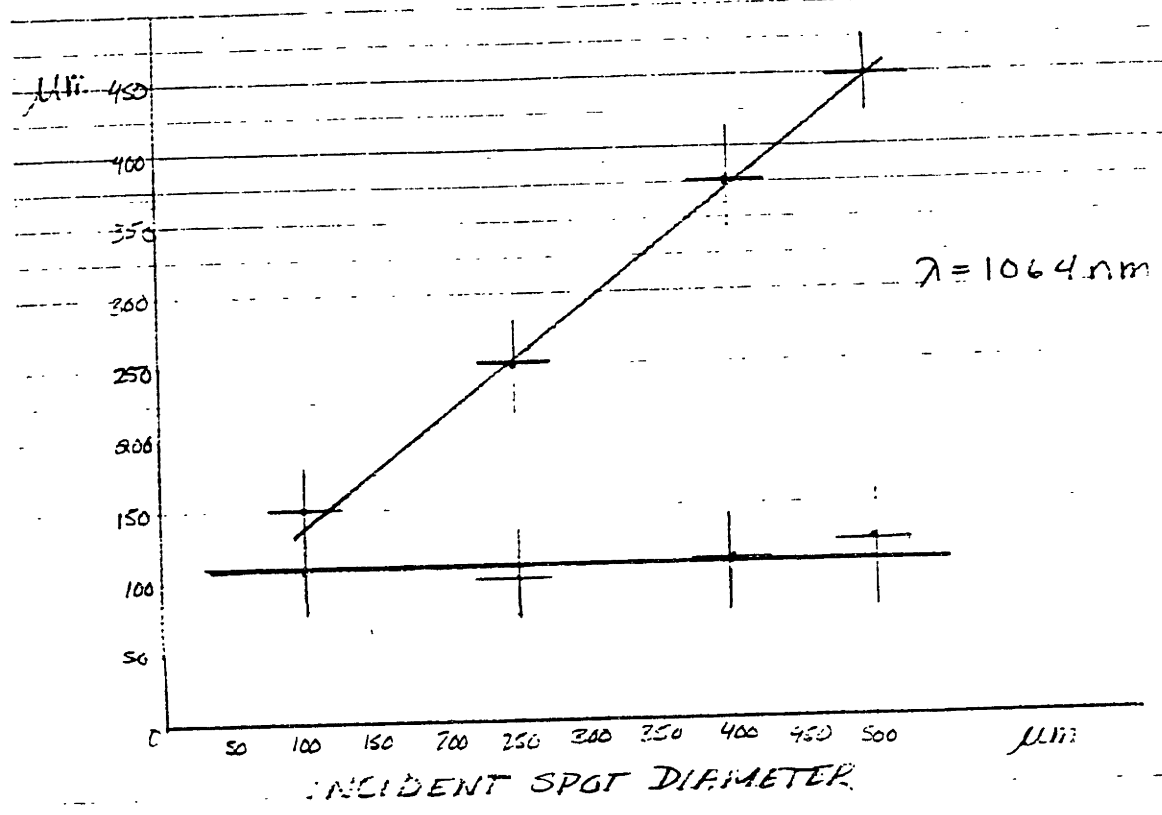
$\lambda = 266\,nm$

DIAMETER

DEPTH

INCIDENT SPOT DIAMETER

FIG.10B   ABLATED DEPTH + DIAMETER
VS INCIDENT SPOT SIZE
CALF ARTERY
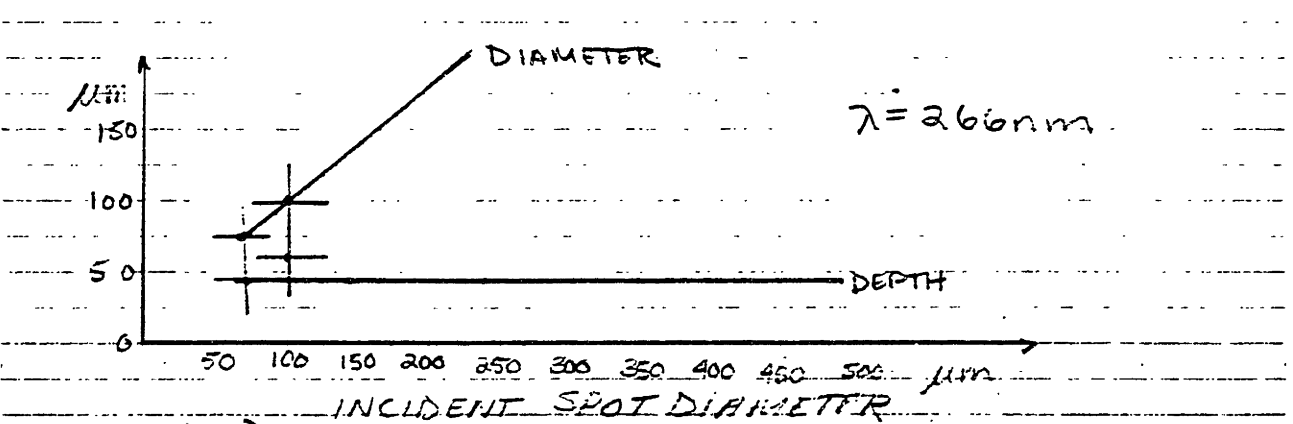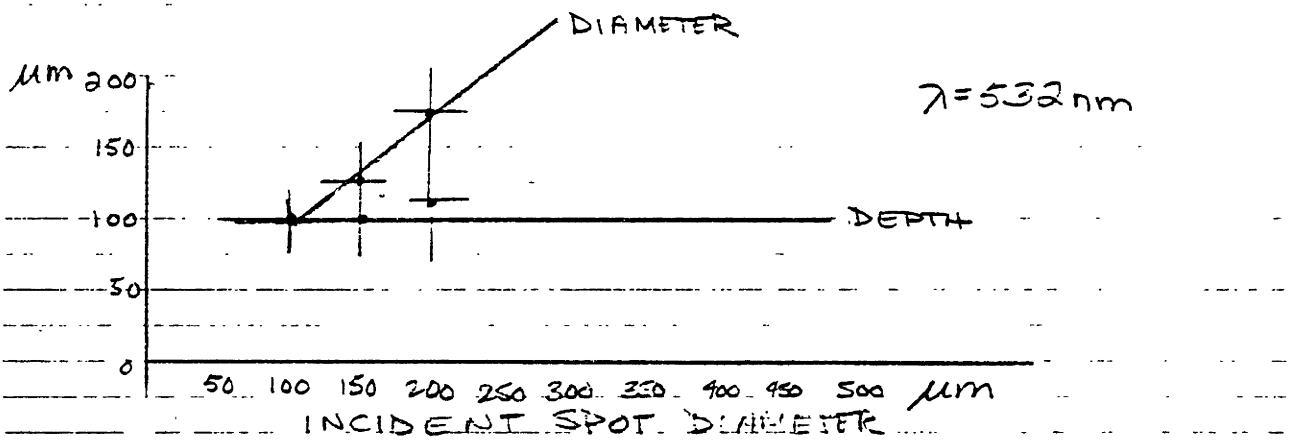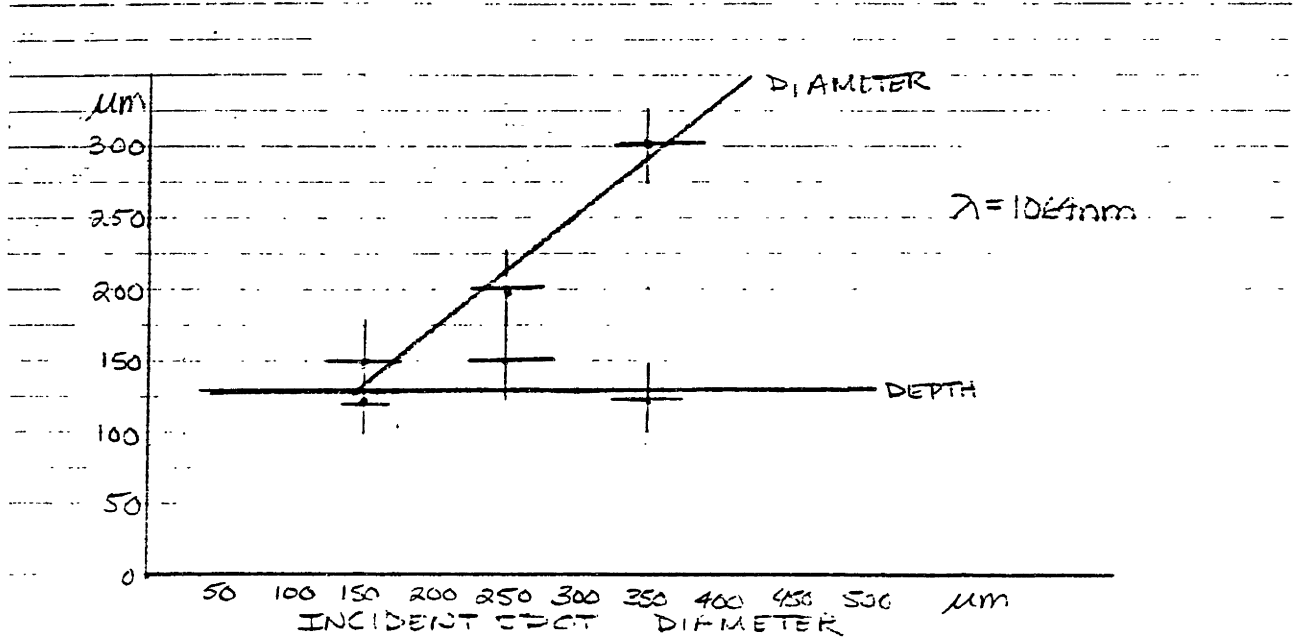
FIG. 10C
ABLATED DEPTH AND DIAMETER
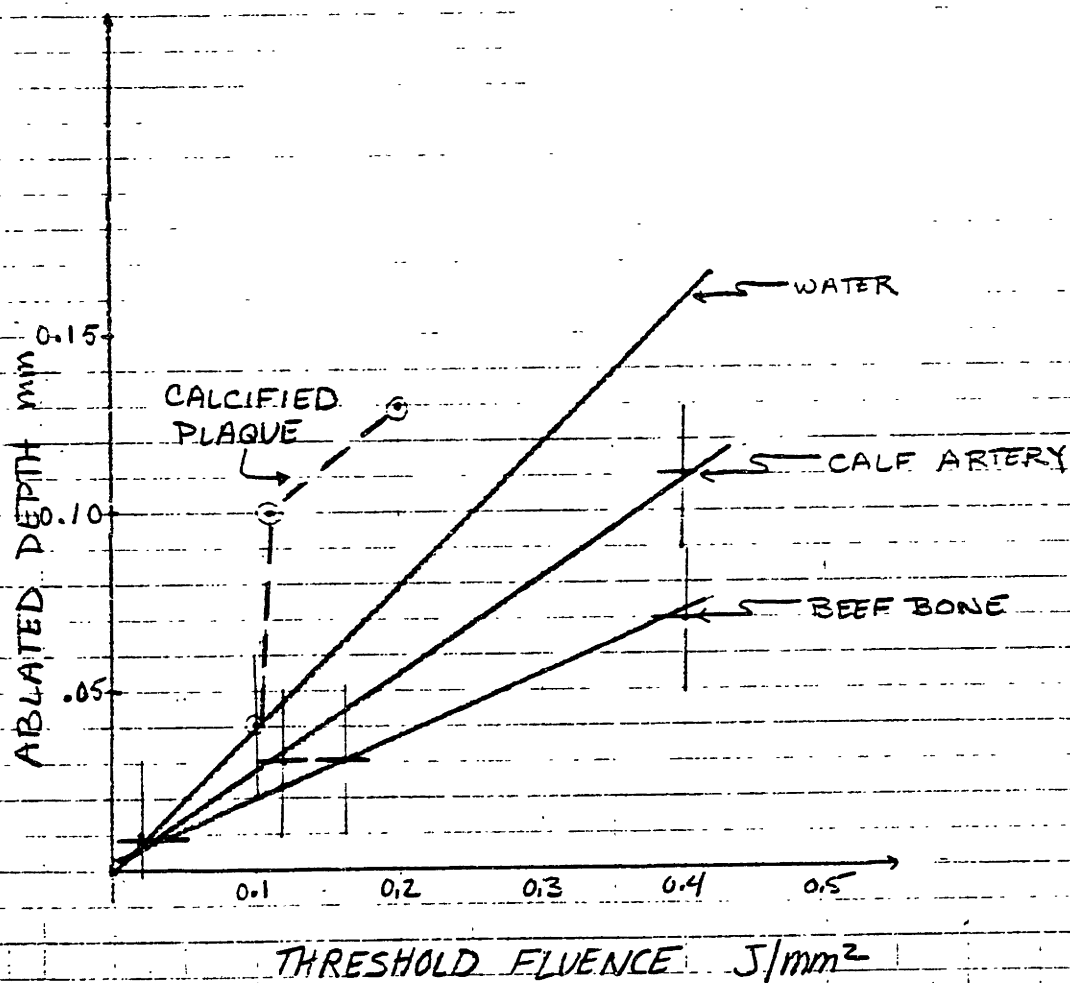VS INCIDENT SPOT DIAMETER

CALCIFIED PLAQUE

FIG. 11   ABLATED DEPTH
VS
THRESHOLD FLUENCE
(asymptotic VALUE)

FIG. 12

SAMPLE	λ(nm)	THRESHOLD FLUENCE J/mm² *	ABLATED DEPTH mm	PENETRATION DEPTH mm	ΔHexp/α J/mm³
CALF ARTERY	266	.02 (.02)	0.01	0.050	2.0
CALF ARTERY	532	.12 (.12)	0.03	0.40	4.0
CALF ARTERY	1064	.4 (.4)	0.1.1	1.0	3.6
BEEF BONE	266	.02 (.01)	.02	0.05	1.0
BEEF BONE	532	.16 (.16)	.03	0.40	5.3
BEEF BONE	1064	.40 (.40)	.06	1.0	6.7
CALCIFIED PLAQUE	266	.10 (.10)	.04	0.05	2.5
CALCIFIED PLAQUE	532	.32 (.11)	0.10	0.40	3.2 (1.1)
CALCIFIED PLAQUE	1064	.25 (.20)	.13	1.0	1.9 (1.5)

*FOR 100 μm diameter spot

in parentheses is the asymptotic value

ΔH for thermal heating of water = 2.5 J/mm²

REFERENCES

1.   American Heart Association, Heart Facts (Dallas: n.p., 1985) pp.4.

2.   D.S.J. Choy, S.H. Stertzer, H.Z. Rotterdam, M.S. Bruno, "Laser Coronary Angioplasty: Experience with 9 Cadaver Hearts", Amer. J. Cardiol., vol. 50, pp. 1209, 1982.

3.   G.S. Abela, S., Normann, D. Cohen, R.L. Feldman, E.A. Geiser, C.R. Conti, "Effects of Carbon dioxide, Nd:YAG, and Argon Laser Radiation on Coronary Atheromatous Plaques:, Am. J. Cardiol. vol. 50, pp. 1199-1205, 1982.

4.   J.M. Isner, R.H. Clarke, "Current Status of Lasers in the Treatment of Cardiovascular Disease", IEEE J. Quant. Elec., vol. QE-20, no. 12, pp. 1406-1419, 1984.

5.   S. Trokel, R. Srinivasan, B. Braren, "Excimer Laser Surgery of the Cornea", Am. J. Ophtal., vol.96, pp. 710-713, 1983.

6.   R.J. Lane, R. Linsker, J.J. Wynn, "Ultraviolet-laser ablation of skin", Lasers in Surgery and Medicine, vol. 4, pp. 201-206, 1984.

7.   R.E. Hong, Appl. Phys. Lett. vol.3, no. 8, 1963.

8.   D.W. Fradin, E. Yablonovitch, M. Bass, "Confirmation of an Electron Avalanche Causing Laser-induced Bulk Damage at 1.06 um", Applied Optics, vol. 12, no. 4, pp. 700-709, 1973.

9.   J.F. Ready, The Effets Of High Power Laser Radiation, New York: Academic Press, 1971.

10.   E.S. Bliss, D. Milam, R.A. Bradbry, App. Opt., vol. 12, no. 4, pp. 677-698, 1973.
1972.

11. C.R. Guiliano, Appl. Phys. Lett., vol. 21, pp. 39-41,

12. N. Bloembergen, Appl. Opt., vol. 12, pp. 661-664, 1973.

13. A. Gold, H.B. Beeb, Phys. Rev. Lett., vol. 14, pp. 60, 1965.

14. N. Bloembergen, IEEE J. Quant. Elec., vol. QE-10, no.

3, 1974.

15.   J.F. Ready, The Effets Of High Power Laser Radiation, New York: Academic Press, pp. 213-316, 1971.

16.   A.   Yariv, Quantum Electronics, 2nd Edition, John Wiley& Sons, Inc., pp. 490-498, 1975.

17.   S.A. Ramsden, W.E.R. Davies, Phys. Rev. Lett., vol 13, pp. 227, 1964.

18.   R.D. Bleach, D.J. Nagel, J. App, Phys., vol.49, pp.3832-3841, 1978.

19.   J.F. Ready, The Effets Of High Power Laser Radiation, New York: Academic Press, 1971.

20.   B.M. Ashkinadze et al., Sov. Phys. JETP, vol. 37, 1968.